Inorg. Chem. **1986**, *25*, 1277-1280 **1277**

Contribution from the Department of Chemistry,
The University of Houston—University Park, Houston, Texas 77004

Electrochemical and Spectroelectrochemical Studies of (Tetraphenylporphyrinato)rhodium(III) Acetyl, (TPP)Rh($COCH_3$)

K. M. Kadish,* J. E. Anderson, C.-L. Yao, and R. Guilard[†]

Received August 26, 1985

The oxidations and reductions of (tetraphenylporphyrinato)rhodium(III) acetyl, (TPP)Rh($COCH_3$), were studied by both electrochemical and spectroelectrochemical techniques in benzonitrile and tetrahydrofuran. (TPP)Rh($COCH_3$) undergoes two one-electron reductions, which occur at −1.36 and −1.84 V vs. SCE in benzonitrile, 0.1 M TBAP. The first reduction generates an anion radical of Rh(III) rather than a Rh(II) species. This same compound undergoes three one-electron oxidations, which occur at 1.03, 1.33, and 1.52 V vs. SCE in benzonitrile, 0.1 M TBAP. Similar reduction potentials are observed in THF, but oxidations are beyond the potential range of the solvent. The site of each reduction and oxidation is discussed.

Introduction

The electrooxidation of (P)RhCl and (P)Rh(NO) where P = OEP or TPP has been described.[1] Both series of compounds undergo two reversible oxidations that appear to involve the porphyrin π ring system. Two reversible oxidations are also observed for (TPP)Rh(L)Cl and (TPP)Rh$(L)_2^+Cl^-$, where L is dimethylamine. These electrode reactions also appear to involve the porphyrin π ring system.[2] In contrast the electrochemical reduction of (TPP)Rh(L)Cl and (TPP)Rh$(L)_2^+Cl^-$ involves a Rh(III)/Rh(II) reaction and the electrochemical generation of Rh(II) is followed by a rapid chemical reaction.[2] This leads to an irreversible first-reduction process by cyclic voltammetry. Irreversible one-electron reductions also occur for (TPP)Rh(O_2) as well as for (P)RhX where P = OEP or TPP and X = Cl^- or I^-.[3] In fact, no reversible reductions of Rh(III) porphyrins have ever been reported.

In previous publications we described the electrochemical properties of Fe(III),[4] In(III),[5] and Ga(III)[6] porphyrins that were σ-bonded with an alkyl or aryl group. Reversible reductions were obtained for all of these complexes, and the singly reduced species were extremely stable. Rhodium(III) porphyrins that contain a σ-bonded carbon in the axial position are well-known.[7-20] However, an electrochemical study of σ-bonded Rh porphyrins has not been published and thus it was of some interest to see if reversible reductions could be obtained for these types of complexes. This is indeed the case as we wish to report in this paper, which characterizes the oxidation and reduction of (TPP)Rh($COCH_3$).

Experimental Section

Instrumentation and Methods. IR spectra were measured on a Perkin-Elmer 1330 infrared spectrophotometer. UV-visible spectra were recorded on a Tracor Northern 1710 holographic optical spectrometer/multichannel analyzer. NMR spectra were taken on a Varian FT-80 spectrometer. An IBM Model ED-100 electron spin resonance system was used to record ESR spectra. Cyclic voltammetric and polarographic measurements were carried out with an EG&G Princeton Applied Research Model 174A/175 polarographic analyzer/potentiostat coupled with an EG&G Model 9002A X-Y recorder for potential scan rates less than 500 mV/s or a Tektonix 5111 storage oscilloscope for scan rates equal to or larger than 500 mV/s. Platinum-disk electrodes were used, except in the case of the thin-layer spectroelectrochemical cell, where a platinum-minigrid electrode was used. Potentials were all measured vs. a saturated calomel electrode (SCE) which was separated from the bulk of the solution by a fritted-glass-disk junction. Bulk controlled-potential coulometry was performed on an EG&G Princeton Applied Research Model 174 potentiostat/179 coulometer system, coupled with a Princton Applied Research Model RE-0074 time base X-Y recorder. Thin-layer spectroelectrochemical measurements were made with an IBM 225/2A voltammetric analyzer coupled with a Tracor Northern 1710 spectrometer/multichannel analyzer.

Materials. All solvents used for synthesis were either reagent or chemical grade and were utilized without further purification. For electrochemical or spectroelectrochemical measurements reagent grade benzonitrile (PhCN) was vacuum-distilled over P_2O_5. Spectroscopic grade tetrahydrofuran (THF) was distilled over P_2O_5 followed by distilling over sodium under a nitrogen atmosphere. Tetra-*n*-butylammonium perchlorate (TBAP) was purchased from Eastman Kodak Co., twice recrystallized from ethyl alcohol, and stored in a vacuum oven at 40 °C. Unless otherwise noted, 0.1 M TBAP was used as supporting electrolyte for cyclic voltammetric measurements while 0.2 M TBAP was used for bulk solution electrolysis and spectroelectrochemical measurements.

Table I. Half-Wave Potentials (V vs. SCE) for Oxidation and Reduction of (TPP)Rh($COCH_3$) in PhCN and THF Containing 0.1 M TBAP (Scan Rate 100 mV/s)

solvent	3rd oxidn	2nd oxidn	1st oxidn	1st redn	2nd redn
PhCN	+1.52[b]	+1.33[a]	+1.03	−1.36	−1.84
THF				−1.37	−1.78

[a] Anodic peak potentials of oxidation wave (see Figure 1). [b] This peak corresponds to the oxidation of $[(TPP)Rh^{III}]^{2+}$, which is generated upon cleavage of the Rh–carbon bond.

Synthesis of Compounds. The synthesis and characterization of (TPP)Rh($COCH_3$) has been described by James.[10] (TPP)Rh($COCH_3$) is also recovered as a side product in the synthesis of (TPP)Rh(O_2).[3] Both methods give the same product, and the latter method of synthesis was used predominantly in this study. The produced (TPP)Rh($COCH_3$) was identified by NMR, IR, and UV-visible spectroscopy and agrees with data in the literature.[10] The ν_{CO} band in the IR spectrum is located at 1731 cm^{-1}. The NMR spectrum has the following resonances in $CDCl_3$:

[†] On leave from the Université de Dijon, Dijon, France.

(1) Wayland, B. B.; Newman, A. R. *Inorg. Chem.* **1981**, *20*, 3093.
(2) Kadish, K. M.; Yao, C.-L.; Anderson, J. E.; Cocolios, P. *Inorg. Chem.* **1985**, *24*, 4515.
(3) Kadish, K. M.; Yao, C.-L.; Anderson, J. E., unpublished results.
(4) Lançon, D.; Cocolios, P.; Guilard, R.; Kadish, K. M. *J. Am. Chem. Soc.* **1984**, *106*, 4472.
(5) Kadish, K. M.; Boisselier-Cocolios, B.; Cocolios, P.; Guilard, R. *Inorg. Chem.* **1985**, *24*, 2139.
(6) Kadish, K. M.; Boisselier-Cocolios, B.; Coutsolelos, A.; Mitaine, P.; Guilard, R. *Inorg. Chem.* **1985**, *24*, 4521.
(7) Fleischer, E. B.; Lavallee, D. *J. Am. Chem. Soc.* **1967**, *89*, 7132.
(8) Fleischer, E. B.; Thorp, R.; Venerable, D. *J. Chem. Soc. D* **1969**, 475.
(9) Fleischer, E. B.; Sadasivan, N. *Chem. Commun.* **1967**, 159.
(10) James, B. R.; Stynes, D. V. *J. Chem. Soc., Chem. Commun.* **1972**, 1261.
(11) Ogoshi, H.; Setsune, J.; Yoshida, Z. *J. Chem. Soc., Chem. Commun.* **1975**, 572.
(12) Ogoshi, H.; Setsune, J.; Omura, T.; Yoshida, Z. *J. Am. Chem. Soc.* **1975**, *97*, 6461.
(13) Ogoshi, H.; Setsune, J.; Yoshida, Z. *J. Am. Chem. Soc.* **1977**, *99*, 3869.
(14) Grigg, R.; Grimshaw, J. T.; Viswanatha, V. *Tetrahedron Lett.* **1976**, 289.
(15) Abeysekera, A. M.; Grigg, R.; Grimshaw, J. T.; Viswanatha, V. *J. Chem. Soc. Perkin Trans. 1* **1977**, 36.
(16) Abeysekera, A. M.; Grigg, R.; Grimshaw, J. T.; Viswanatha, V. *J. Chem. Soc. Perkin Trans. 1* **1977**, 1395.
(17) Wayland, B. B.; Woods, B. A. *J. Chem. Soc., Chem. Commun.* **1981**, 700.
(18) Wayland, B. B.; Woods, B. A.; Pierce, R. *J. Am. Chem. Soc.* **1982**, *104*, 302.
(19) Wayland, B. B.; Duttaahmed, A.; Woods, B. A. *J. Chem. Soc., Chem. Commun.* **1983**, 142.
(20) Cohen, I. A.; Chow, B. C. *Inorg. Chem* .**1974**, *13*, 488.

0020-1669/86/1325-1277$01.50/0 © 1986 American Chemical Society

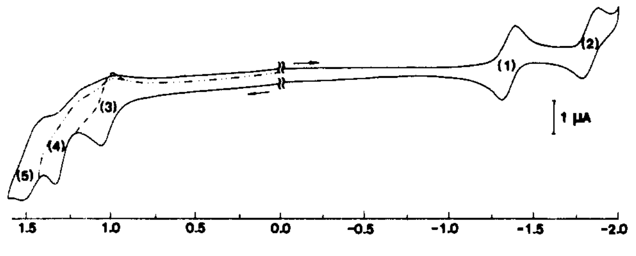

Figure 1. Cyclic voltammograms of 8.8 × 10^{-4} M (TPP)Rh($COCH_3$) in PhCN, 0.1 M TBAP (scan rate 0.1 V/s).

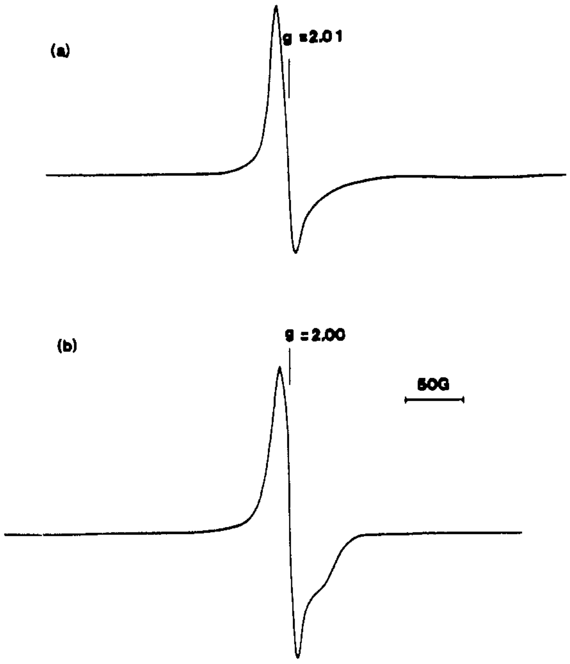

Figure 2. ESR spectra of (a) singly reduced (TPP)Rh($COCH_3$) and (b) singly oxidized (TPP)Rh($COCH_3$) at 123 K in PhCN, 0.2 M TBAP.

δ 8.85 (py H, singlet, 8 H), 8.24 (phenyl H, quintet, 8 H), 7.84 (phenyl H, triplet, 12 H), -2.69 (methyl H, singlet, 3 H). The two main peaks in the electronic spectra of the complex in $CHCl_3$ are at 415 and 520 nm, while in pyridine they shift to 420 and 531 nm.

Results and Discussion

Electrochemistry of (TPP)Rh($COCH_3$). The cyclic voltammogram of (TPP)Rh($COCH_3$) has two reductions and three oxidations in benzonitrile, as shown in Figure 1. In THF no oxidations are observed due to the limited oxidation window of this solvent, but two reductions are observed whose potentials are shifted only slightly from those measured in benzonitrile. These oxidation and reduction potentials are presented in Table I.

Similar reductive behavior is observed in benzonitrile and in THF. The first reduction of (TPP)Rh($COCH_3$) occurs at -1.36 V in benzonitrile (Figure 1, peak 1) and gives a reversible, diffusion-controlled, one-electron-transfer peak in both solvents. This is demonstrated by a potential separation of 60 ± 5 mV between the anodic and cathodic peaks, an $E_p - E_{p/2} = 60 \pm 5$ mV, and an $i_p/v^{1/2}$ value equal to a constant. The number of electrons transferred in the first reduction was found to be 1.0 ± 0.1 by current integration. The second reduction of (TPP)Rh($COCH_3$) is also a reversible one-electron-transfer process and occurs at -1.84 V in benzonitrile (Figure 1, peak 2). The peak separation is 60 ± 10 mV, and $E_p - E_{p/2}$ is 60 ± 10 mV. The ratio $i_p/v^{1/2}$ is constant with increase in scan rate, which also suggests a diffusion-controlled electron transfer.

Figure 2a shows the ESR spectrum obtained from a frozen PhCN solution after the first reduction. The reduction was performed at $E_{app} = -1.65$ V. This potential is 290 mV beyond the first reduction potential of (TPP)Rh($COCH_3$) and thus produces the singly reduced complex. As seen in Figure 2a there is a strong signal at $g = 2.01$.

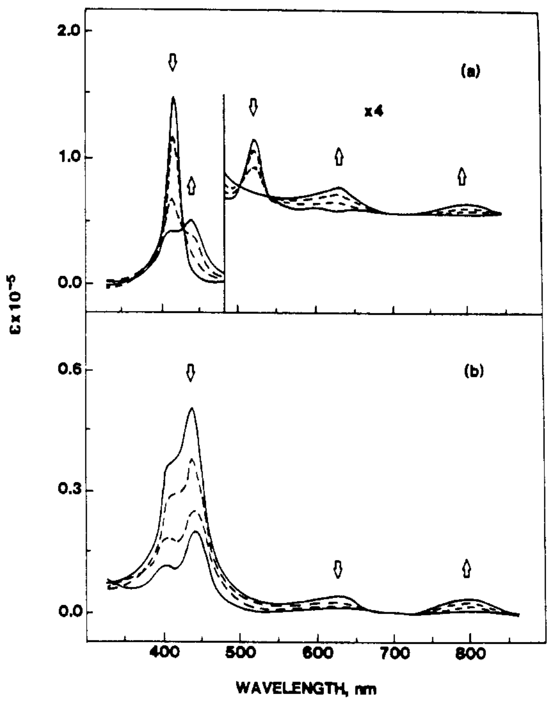

Figure 3. Electronic absorption spectra of (a) neutral and singly reduced and (b) singly and doubly reduced (TPP)Rh($COCH_3$) in PhCN, 0.2 M TBAP.

Table II. UV-Visible Spectra of Oxidized and Reduced (TPP)Rh($COCH_3$) in Benzonitrile

electrode reacn	λ_{max}, nm ($\epsilon \times 10^{-3}$)			
none	417 (147)	522 (11.8)	549 (1.9)	
1st redn	441 (50.9)	630 (4.5)	790 (1.1)	900 (3.6)
2nd redn	446 (22.1)	630 (0.7)	794 (2.2)	
1st oxidn[a]	422 (136)	440 (sh)	533 (8.9)	568 (2.4)

[a] Spectrum is that of electrogenerated (TPP)$RhClO_4$. All further oxidations (in Figure 1) are of this species.

The changes that occur in the electronic absorption spectrum of (TPP)Rh($COCH_3$) after the first reduction are shown in Figure 3a, and a summary of the maximum absorption band positions and molar absorptivities in benzonitrile is presented in Table II. During reduction, the Soret band at 417 nm drops dramatically in intensity and a new band appears at 441 nm. There is an isosbestic point at 431 nm. New absorption peaks are observed at 630, 790, and 900 nm and suggest the formation of an anion radical of Rh(III). This reduction is reversible, as demonstrated by the fact that the original electronic absorption spectrum is regenerated upon reoxidation of the singly reduced species.

The electronic absorption spectrum after the second reduction of (TPP)Rh($COCH_3$) is shown in Figure 3b. After addition of a second electron the Soret band further decreases in intensity as does the band at 630 nm. A new band appears at 794 nm. This reduction is not reversible on the spectroelectrochemistry time scale, and if the second reduction product is reoxidized at -1.64 V, the singly reduced species is not spectroscopically observed. This indicates that the second reduction is only reversible on the electrochemical time scale (1-5 s) and that a chemical reaction occurs after the addition of a second electron to (TPP)Rh($COCH_3$).

An ESR spectrum was also obtained from a frozen benzonitrile solution after controlled-potential reduction at -1.95 V. The doubly reduced (TPP)Rh($COCH_3$) was expected to be diamagnetic, and the *g* value of 2.00 appears to be that of a free radical. The intensity of the ESR signal is relatively low, but it is re-

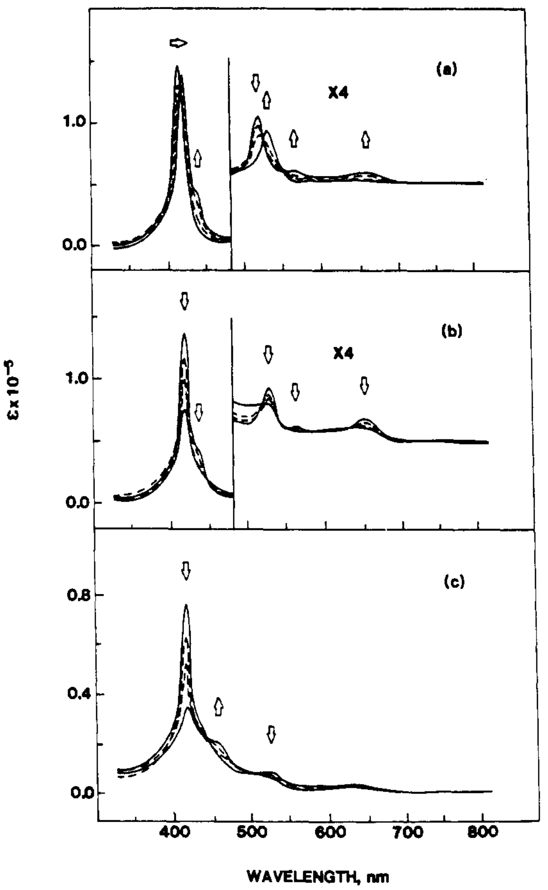

Figure 4. Electronic absorption spectra of (a) neutral and singly oxidized, (b) singly and doubly oxidized, and (c) doubly and triply oxidized (TPP)Rh($COCH_3$) in PhCN, 0.2 M TBAP.

producible. Most likely, this ESR signal results from a small amount of (TPP)Rh($COCH_3$) decomposition, which leads to the formation of a free radical.

The first oxidation of (TPP)Rh($COCH_3$) occurs at +1.03 V in benzonitrile and gives a reversible one-electron, diffusion-controlled process by cyclic voltammetry. This is demonstrated by an $E_p - E_{p/2} = 60 \pm 10$ mV, a peak separation of 60 ± 10 mV, and a constant value of $i_p/v^{1/2}$ (see Figure 1). The global number of electrons transferred in this oxidation was measured to be 1.0 ± 0.1 by controlled-potential coulometry.

Figure 4a and Table II show the changes that occur in the electronic absorption spectrum upon controlled-potential oxidation of (TPP)Rh($COCH_3$) at +1.2 V. After the abstraction of one electron, the Soret band shifts to 422 nm. There is a shoulder at 440 nm, and new bands appear at 533 and 568 nm. The original electronic absorption spectrum is not regenerated upon reduction of the first oxidation product, indicating a reversibility only on the electrochemical time scale. The spectrum of the first oxidation product suggests formation of (TPP)$Rh^{III}ClO_4$.

The second oxidation of (TPP)Rh($COCH_3$) occurs at $E_p = 1.33$ V in benzonitrile (Figure 1, peak 4). It is an irreversible process, as seen by the lack of a return peak in the cyclic voltammogram. In addition, if the cyclic voltammogram is scanned past the second oxidation peak, no return peak is observed for the first oxidation. This is indicative of one or more chemical reactions that follow the second oxidation.

The electronic absorption spectrum of the second oxidation product (Figure 4b) indicates that the electron is removed from the porphyrin π ring system. There is a drop in the Soret band intensity at 442 nm as well as a decrease in the bands at 533 and 658 nm. Reduction of the second oxidation product at 0.00 V does not regenerate the starting compound, demonstrating the irreversible nature of the second oxidation. As will be shown in the following sections, this oxidation leads to $[(TPP)RhClO_4]^+$ as the final species.

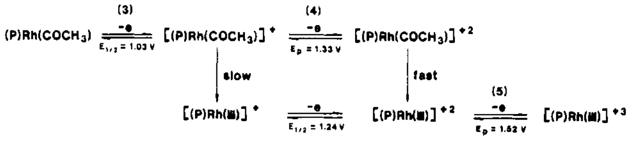

Figure 5. Mechanism for the oxidation of (TPP)Rh($COCH_3$) in PhCN.

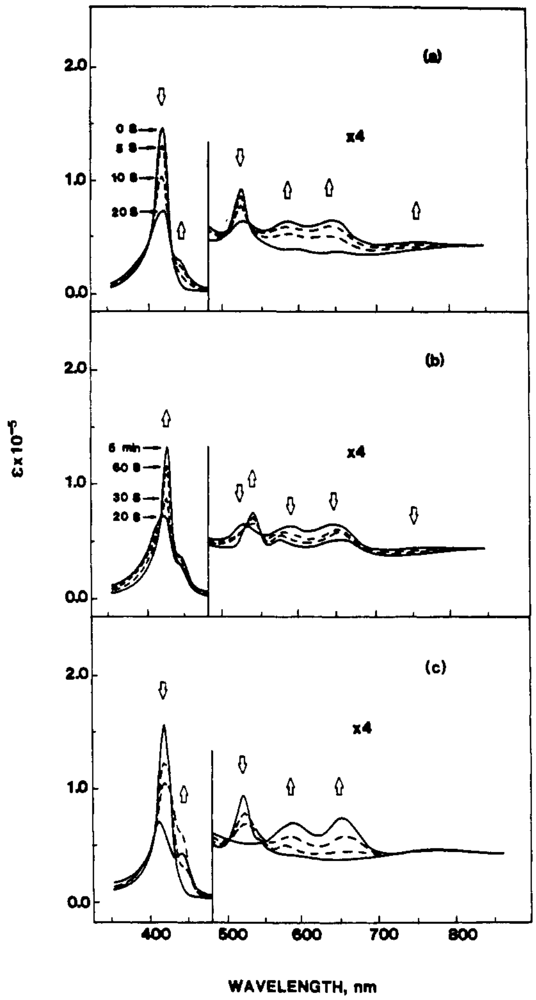

Figure 6. Thin-layer spectra obtained for oxidized (TPP)Rh($COCH_3$) in PhCN, 0.2 M TBAP (a) during the first 20 s of electrolysis at +1.2 V; (b) during continued electrolysis at +1.2 V from 20 s to 5 min. For (c) the same solution as in (a) plus 1 equiv of (TBA)Cl was used.

The third oxidation of (TPP)Rh($COCH_3$) (Figure 1, peak 5) occurs at $E_p = 1.52$ V in benzonitrile and is an irreversible process. The electronic absorption spectrum (Figure 4c) is consistent with formation of the $[(TPP)RhClO_4]^{2+}$ dication. All absorption bands drop in intensity, and a shoulder on the Soret band appears at 450 nm.

The above results suggest the mechanism shown in Figure 5. On the cyclic voltammetric time scale reactions 3 and 4 (Figure 1) correspond to successive one-electron abstractions from (TPP)Rh($COCH_3$). The singly and doubly oxidized species are unstable, and cleavage of the acetyl group results. This is shown in eq 1 for the case of electrogenerated $[(TPP)Rh(COCH_3)]^+$.

$$[(TPP)Rh(COCH_3)]^+ \rightarrow [(TPP)Rh^{III}]^+ + [COCH_3]\cdot \qquad (1)$$

A similar mechanism occurs for (P)In(R)[5] and (P)Ga(R),[6] where three oxidations are observed, the first of which involves cleavage of the metal–carbon bond. After cleavage of the rhodium–carbon bond the generated (TPP)Rh^{III} (or (TPP)$RhClO_4$) is then oxidized by two additional one-electron transfers. The first of these occurs at 1.24 V, and the second (reaction 5, Figure 5) at 1.52 V. These potentials are positively shifted from the values of 0.98 and 1.36

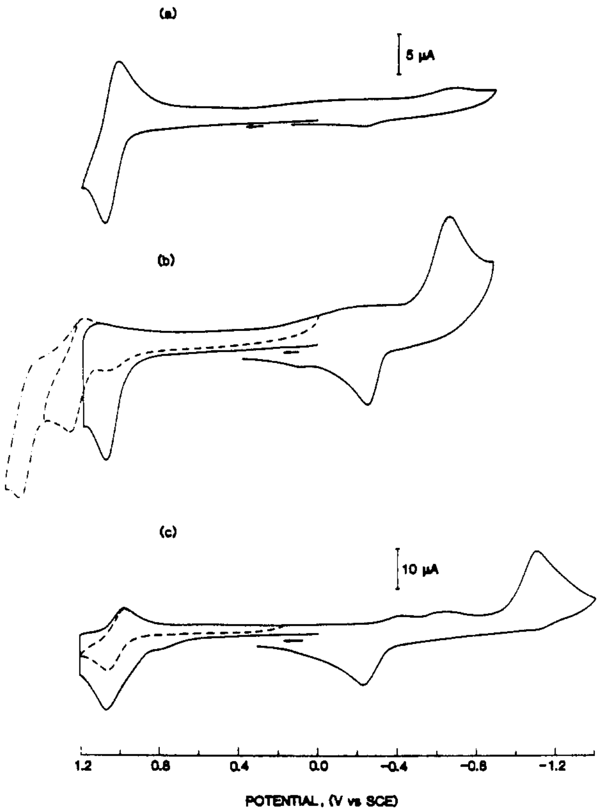

Figure 7. Thin-layer cyclic voltammogram of (TPP)Rh($COCH_3$) in PhCN, 0.2 M TBAP: (a) single scan from +1.2 to −1.0 V at 10 mV/s; (b) same solution but the potential held at 1.2 V for 5 min and then scanned in a negative direction (solid line) or a negative and then a positive direction (dashed line); (c) same conditions as in (a) but the solution contained 1 equiv of Cl^-. The dotted line on the second oxidative scan corresponds to the (TPP)RhCl/[(TPP)RhCl]$^+$ couple.

V for oxidations[1] of (TPP)RhCl.

Further evidence for formation of [(TPP)Rh^{III}]$^+$ as shown in Figure 5 is provided by time-resolved thin-layer spectroelectrochemistry in the presence and absence of chloride ion. The Soret band molar absorptivity decreases as [(TPP)Rh($COCH_3$)]$^+$ is generated during the first 20 s of electrolysis at +1.2 V in PhCN, 0.2 M TBAP (Figure 6a). However, within 20 s, a significant amount of Rh–carbon bond cleavage begins to occur and the (TPP)$RhClO_4$ spectrum is generated. This is shown in Figure 6b. The Soret band increases in intensity, and the final spectrum is similar to that of [(TPP)Rh^{III}]$^+$ species. Finally, in the presence of 1 equiv of Cl^-, (TPP)RhCl is formed almost instantaneously after oxidation, and at a potential of +1.2 V, this species is then oxidized to give [(TPP)RhCl]$^+$. This is shown in Figure 6c, where direct conversion of (TPP)Rh($COCH_3$) to [(TPP)RhCl]$^+$ is monitored.

Similar mechanistic conclusions are obtained from thin-layer cyclic voltammograms in the presence and absence of Cl^-. The thin-layer voltammogram of (TPP)Rh($COCH_3$) in 0.2 M TBAP is shown in Figure 7a. At a scan rate of 10 mV/s a well-defined first-oxidation peak is obtained at $E_{1/2}$ = 1.03 V and two small peaks are seen at E_{pc} = −0.67 V and E_{pa} = −0.24 V. In contrast, if the potential is held at +1.18 V for 5 min, a complete conversion to (TPP)$RhClO_4$ occurs. Under these conditions, new oxidations are observed at +1.24 and +1.52 V and large coupled reduction/oxidation peaks occur at E_p = −0.67 and −0.24 V (Figure 7b). These last peaks correspond to the irreversible reduction of (TPP)$RhClO_4$ and a reoxidation of the generated Rh(II) species. This type of mechanism has been discussed in a previous pubication.[2] Finally, in the presence of Cl^-, the generation of (TPP)RhCl and its oxidation to [(TPP)RhCl]$^+$ are evident. A second oxidation cycle (Figure 7c) shows a reversible couple at 0.97 V, which corresponds to (TPP)RhCl/[(TPP)RhCl]$^+$. At the same time, the irreversible reduction peak of (TPP)RhCl has shifted to −1.10 V. No change is observed in the oxidation peak at −0.24 V, indicating conversion to the same Rh(II) species after initial electroreduction.[2]

The ESR spectrum of the first oxidation product after 1.5 min of controlled-potential electrolysis is shown in Figure 2b. It is asymmetric and has a broad tail with a *g* value of 2.00. Continued controlled-potential electrolysis yielded a decrease in the intensity of the initial signal, which completely disappeared after 60 min of electrolysis. Since [(TPP)Rh^{III}]$^+$ is diamagnetic, this suggests that the initially observed signal corresponds primarily to that of [(TPP)Rh($COCH_3$)]$^+$ before cleavage of the metal–carbon bond. Finally, a strong ESR signal is obtained after controlled-potential oxidation of (TPP)Rh($COCH_3$) at 1.4 V. This signal has a value of 2.00 and is assigned as due to the generated [(TPP)Rh^{III}]$^{2+}$ species, as shown in Figure 5.

In summary, (TPP)Rh($COCH_3$) has a much different electrochemical behavior than (TPP)RhCl, (TPP)Rh(NO), (TPP)Rh(O_2), (TPP)Rh$(L)_2{}^+Cl^-$, or (TPP)Rh(L)Cl. A major difference is that the site of the first reduction of (TPP)Rh($COCH_3$) does not involve the metal center. For Rh(III) porphyrins complexed with amines or halide ions the first reduction is metal-centered and leads to a Rh(II) species that quickly reacts chemically.[2] Apparently, the acetyl group either prevents the formation of a Rh(II) species or blocks the dimerization process. In either case it is clear this is the direct result of the metal–carbon bond.

Acknowledgment. The support of the National Science Foundation (Grant No. 8215507) is gratefully acknowledged.

Registry No. TBAP, 1923-70-2; (TPP)Rh($COCH_3$), 40844-52-8; [(TPP)Rh($COCH_3$)]$^+$, 100908-94-9; [(TPP)Rh($COCH_3$)]$^{2+}$, 100908-97-2; (TPP)$RhClO_4$, 100908-95-0; [(TPP)$RhClO_4$]$^+$, 100908-92-7; [(TPP)$RhClO_4$]$^{2+}$, 100908-93-8; (TPP)RhCl, 77944-60-6; [(TPP)RhCl]$^+$, 100908-96-1; Cl^-, 16887-00-6; Rh, 7440-16-6.